CLC of waste-derived fuel and biomass in a 150-kW pilot unit

Øyvind LANGØRGEN[1]*#, Inge SAANUM[1], Roger KHALIL[1], Nils Erland L. HAUGEN[1]

[1] SINTEF Energi AS (SINTEF Energy Research), Trondheim, Norway

*Corresponding Author, oyvind.langorgen@sintef.no, #Presenting Author

Abstract – In this work, solid recovered waste-derived material (SRF) and biomass are converted in the 150-kW_{th} CLC pilot unit at SINTEF Energy Research in Norway, using ilmenite as an oxygen carrier. The very first tests show that SRF and the biomass reference fuel seem to behave rather similar with respect to fuel reactor gas conversion efficiency and CO_2 capture rate. Two tests with biomass and one with SRF have been performed, and they all show high capture rates, about 98 %. FR gas conversion efficiency is also rather similar, though, not higher than about 70%. In earlier biomass tests in the same unit, a FR gas conversion efficiency of about 80 % was achieved, with ilmenite particles of smaller size. What seems to be the largest difference between the two fuels is the FR carbon conversion (i.e., the percentage of carbon fed with the fuel that is leaving the FR in gaseous form), which is significantly lower for the SRF. This means more carbon particulates are leaving the FR in the SRF case, and since the capture rate is high, they are not passed to the AR but seems to leave with the FR exhaust gas in larger amount than for the biomass case. Both fuels used were in the form of pellets with 8 mm diameter. The fuel feed rate was 19.5 kg/h for all cases, equivalent to 103 kW for the biomass case, and 111 kW for the SRF case. Operation with biomass and SRF is attractive since they can both contribute to negative CO_2 emissions due to the biogenic carbon content. Combustion of such fuels in standard fluidized bed furnaces is a commercially available technology. This work is a first test to investigate how waste-derived materials will behave in the 150-kW_{th} fluidized bed CLC system at SINTEF Energy Research. The pilot unit does not include a carbon stripper. Another aspect with the tests is therefore to verify if such a system simplification still can provide a high capture rate. For reactive fuels, such as SRF and biomass, the presented tests show that this might be achieved.

1 Introduction

Most scenarios consistent with reducing CO_2 emissions to net zero by 2050, and limit long-term global temperature increase to 1.5 °C, include CO_2 capture, utilization, and storage (CCUS) as one of several important measures. The IPCC analyzed many scenarios meeting these emissions targets, showing CO_2 capture by 2050 in the range 5.5 – 18.5 billion tonnes CO_2 per year ($GtCO_2$ per year) [1]. The more recent Net-Zero Emissions scenario from IEA estimates a somewhat lower value with a total CO_2 capture of 7.6 $GtCO_2$ per year by 2050 [2]. In any case, these scenarios show that a massive increase in CO_2 capture is needed compared to the present value of about 0.04 Gt CO_2 per year being captured by the 27 commercial operational CCS facilities worldwide [3].

Importantly, a large share of the needed CCS capacity will be allocated to carbon dioxide removal (CDR) technologies. The two main approaches to CDR are: bioenergy with carbon

capture and storage (BECCS) and direct air carbon capture and storage (DACCS), where BECCS plays the dominant role. The IPCC scenarios include a very large share of CDR capacity, in the range 3.5 - 16 Gt CO_2/year in 2050 [1], while the IEA prescribes a lower CDR value of 1.9 Gt CO_2 captured and stored per year by 2050 [2]. Still, this is a large number since in average it involves as many as 1900 plants, each capturing one million tonnes of biogenic CO_2 per year.

Most waste fractions being incinerated in waste-to-energy (WtE) plants do generally contain significant amounts of biogenic carbon, often in the range 40–50 % of the carbon content. When CCS is added to such plants, they will contribute to the needed CDR capacity. WtE plants generate energy in form of power and/or heat from waste fractions that most often cannot be used for other purposes. In that respect, they do not share the same challenges as biomass related to sustainability and potential other usage. WtE with CCS is therefore an interesting technology to develop and deploy, being partly a BECCS technology.

Chemical Looping Combustion (CLC) is a possible BECCS technology that can provide negative CO_2 emissions at relatively high efficiency and low cost [4]. This is of particular interest considering the large extent of carbon dioxide removal incorporated in many emission scenarios. Several studies show that CLC technology can achieve low energy penalty for CO_2 capture. Net electric efficiency penalties of only 2.5 and 4 %-points compared to relevant reference technology without CO_2 capture has been reported using coal as fuel ([5], [6]). Net electric efficiency penalty is also shown to be lower than other comparable technologies with CO_2 capture, with 5 %-points gain compared to an oxyfuel CBF case [5], and 6.5 %-points gain compared to a CFB with MEA absorption [7], the latter study using petcoke as fuel. At the same time, both studies showed much higher CO_2 capture rate for the CLC cases than the reference capture technologies.

The low energy penalty of the CLC process, together with high capture rate, is beneficial to the economy of the process and the resulting cost of CO_2 avoided, electricity and heat. A CO_2 avoidance cost of less than 26 €/tonne has been estimated in an earlier study [6], using coal as fuel and utilizing as much as possible the similarities between standard circulating fluidized bed (CFB) technology and fluidized bed based CLC technology. In a robust decision-making study [8] it was investigated under which assumptions a Bio-CLC CHP plant would be a profitable investment when providing heat for the Helsinki district heating system and electricity for the Nordic electricity market. The Bio-CLC plant had a 50 % chance to be profitable (> 10 % internal rate of return) if it can get a net income from the captured biogenic CO_2 of at least 10 €/tonne. The net income is a lump value incorporating both incomes, subsidies and costs related to the CO_2. Today, this value is negative since there is zero incomes and subsidies for negative emissions through capture of biogenic CO_2, while there will be a cost related to CO_2 transport and storage.

The CLC process has, during the last two decades, been operated in nearly 50 smaller CLC lab and pilot units in the range 0.3 kW_{th} to 1 MW_{th} for totally more than 11 000 hours using different fuels, both gaseous and solid fuels, and different oxygen carrier materials [9]. During the last 15 years, significant developments have been made especially in CLC of solid fuels, and about 20 lab- and pilot units have reported results [10]. More recently, a 3 MW_{th} demo unit is under construction in China, as part of the EU-China cooperating project "CHEERS" [11]. The units

are most often based on fluidized bed technology that can make use of many similarities with commercially available technology. Oxygen carriers using low-cost materials such as natural minerals are widely used, with ilmenite as one of the most common. High temperatures and high solid inventory are desirable to reach high CO_2 capture rates. In addition, a carbon stripper between the fuel and air reactor is normally employed in CLC of solid fuels to achieve capture rates close to 100 % [10]. The use of a carbon stripper is most important for solid fuels with low reactivity since they require long residence time for gasification [12].

CLC using biomass has been studied less than CLC with coal, but an increasing number of studies are now available. Bio-CLC can draw on experience from conventional fluidized bed combustion technology for biomass, which is commercially available at large scale and has been utilized for many years, either with 100 % biomass firing, or co-firing with coal [13] or other fuels. Nanjing University operated a 10 kW$_{th}$ CLC pilot plant with sawdust [14], while CSIC investigated CLC of forest and agricultural residues in a 0.5 kW$_{th}$ unit [15]. Chalmers University has performed tests in both a 10 kW$_{th}$ and a 100 kW$_{th}$ pilot unit with different biomass fuels such as biochar and crushed wood pellets [16], using a manganese ore as oxygen carrier yielding gas conversion > 90% and carbon capture > 95%. TU Darmstadt operated their 1 MW$_{th}$ pilot plant with mixtures of coal and torrefied biomass [17]. CLC of biomass was the main technology in the recent Nordic research project "Negative CO_2 Emissions with Chemical Looping Combustion of Biomass" using CLC pilot units of up to 150 kW$_{th}$ size, plus a larger semi-commercial CFB unit of up to 4 MW$_{th}$ biomass feed [4]. SINTEF Energy Research (Norway) has demonstrated CLC operation with biomass at a feed rate of up to 140 kW$_{th}$, using ilmenite as oxygen carrier [18].

CLC of solid waste material fractions has, to our knowledge, not yet been tested. However, conventional fluidized bed combustion of waste is done at commercial scale ([19], [20], [21]). Waste material fractions as RDF (refuse-derived fuel) and SRF (solid recovered fuel) have gone through some pre-treatment for size reduction, mixing and homogenization, and are well suited for fluidized bed operation in that respect [20]. The same reference also points to the main challenges for waste combustion in fluidized beds, as agglomeration, fouling and corrosion issues. The main cause is alkali compounds in the waste feed, with Na and K playing the leading role.

In this study we present results from our very first CLC pilot unit tests with a waste fraction traded as solid recovered fuel (SRF). Ilmenite has been used as oxygen carrier and biomass has been used as a reference fuel for comparison. The tests have been performed in the 150 kW$_{th}$ unit at SINTEF Energy Research. This unit does not contain a carbon stripper and it is of interest to see if this simplified design can manage high enough CO_2 capture rates when operating on reactive fuels, such as biomass and SRF waste.

2 Experimental

2.1 Reactor system and design

The CLC reactor system consists of two interconnected circulating fluidized bed reactors as shown in Figure 1. Both the air reactor (AR) and the fuel reactor (FR) are 6 m tall of which the

first 1 m is a conical bottom section. The remaining 5 m cylindrical sections have internal diameters of 230 mm (AR) and 154 mm (FR). The metal oxide particles circulate between the reactors via the cyclones and loop-seals. In addition, particles are also transferred from the fuel reactor to the air reactor through the lifter, which is fed from the bottom of the fuel reactor. This allows some more flexibility with respect to fluidization velocity and fluidization mode. The system is originally designed for operation on methane as fuel gas at a maximum fuel power of 150 kW$_{th}$ ([22], [23]) and has later been modified to solid fuel feeding [18].
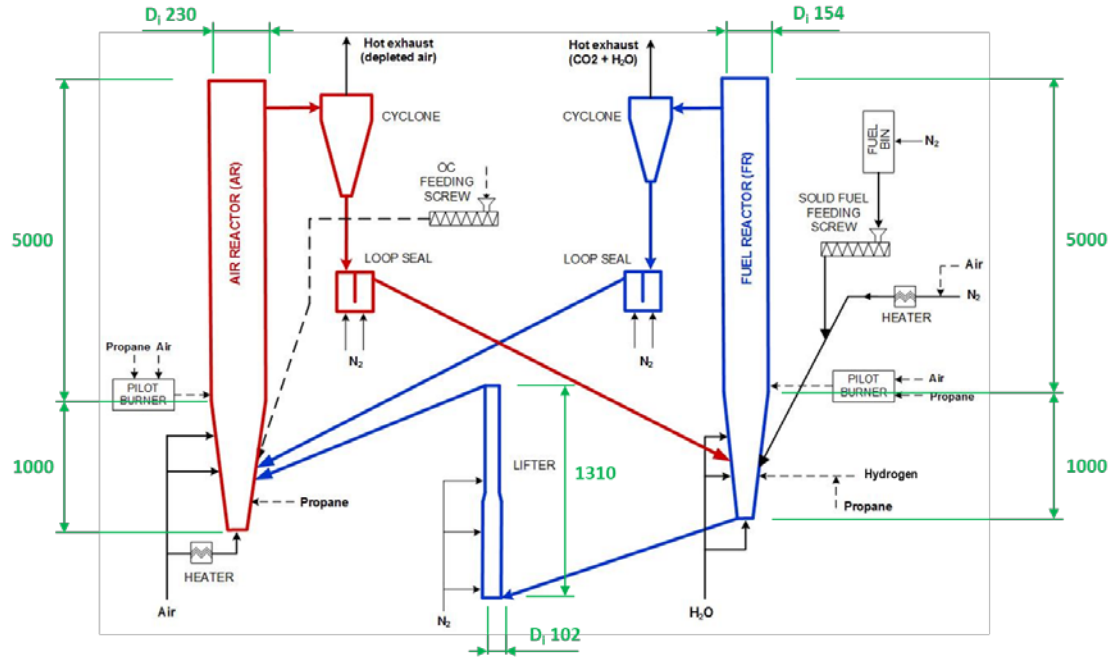
Figure 1: Overview of the 150 kW$_{th}$ CLC reactor system.

The system has a solid fuel feeding screw from which the fuel particles fall into the fuel inlet pipe and are injected into the FR with N2 as a fuel carrying gas. There is an oxygen carrier feeding screw that makes it possible to refill particles to the AR during operation.

During startup, both reactors are heated by 30 kW electric air heaters plus propane and hydrogen fuel gas that are introduced into the particle beds. Pilot burners are mounted above the bed to ensure safe ignition of the injected heat-up fuel. When appropriate temperature levels are reached, injection of solid fuel commence while air to the FR is gradually decreased to zero, after which full CLC operation is reached.

Under normal CLC operation, the reactor temperature is controlled by the CLC process itself, i.e., it is running under auto-thermal operation, including preheating of the primary air to the air reactor. Autothermal operation of a reactor in this small scale is challenging because of the high relative heat loss. To remedy this, much effort has been made in insulating the reactor system well, and the reactor pipes are placed close together for a compact design with small outer surface area.

Each reactor has six pressure transmitters mounted up along the reactor height, with most of them in the bottom part. There are also pressure recordings in the bottom and top of the lifter, out of the cyclones, in the loop-seals as well as in the main air and steam supply lines. There are five temperature transmitters in each reactor, plus temperature measurements in the lifter,

in the exhaust system and in each of the pre-heated inlet streams and in the fluidization steam line to the FR.

The composition of the outlet exhaust gas streams from the cyclones are monitored with on-line gas analyzers. The CO_2, CO and O2 concentrations of the fuel reactor exhaust is measured with an Emerson Rosemount X-stream IR analyzer. A Varian CP4900 Micro-GC is also connected to the fuel reactor exhaust. It measures gases such as H2, CH4, N2, C2 hydrocarbons and helium. Helium is fed to the fuel reactor as a trace gas and its concentration in the exhaust is used for mass balance evaluation. The Micro-GC also measures CO_2 and CO and therefore serves as a check of the IR analyzer. The air reactor gas outlet is monitored with a Horiba PG-250 IR analyzer, measuring CO_2, CO and O2 concentrations.

2.2 Fuels

The reference fuel is biomass from Arbaflame, delivered as pellets with 8 mm diameter. This is a steam-exploded biomass with a brownish color that is less sticky than standard white wood pellets. It has been tested as whole pellets, milled, and sieved, and milled and un-sieved (cf. Figure 2). The composition and combustion data are given in Table 1.

Figure 2: Wood pellets. 8 mm pellets (left); milled and sieved > 800 µm (mid); milled and un-sieved (right).

Table 1: Biomass composition (wt-%), Φ_0, and lower heating value. All values based on fuel as received (a.r.).

C	H	O	N	S	Moisture	Ash	Φ_0 [*]	LHV (MJ/kg)
50.7	5.8	38.1	0.01	0.001	4.9	0.5	1.06	19.0

(*) the molar amount of O2 needed for full conversion of the fuel per mole of carbon in the fuel

The SRF waste was delivered as 8 mm and 16 mm diameter pellets, as well as in loose form. Feeding in loose form would have been beneficial since this material is more easily available than pelletized. However, from fuel feed tests it was clear that 8 mm SRF pellets was the only alternative that could give a stable fuel feed rate with the current feeding system. The different SRF wastes are shown in Figure 3, and composition and combustion data are given in Table 2.

Figure 3: SRF waste. Loose form (left); 16 mm pellets (mid); 8 mm pellets (right).

Table 2: SRF composition (wt-%), Φ_0, and lower heating value. All values based on fuel as received (a.r.).

C		H	O	N	S	Cl	Moisture	Ash	Φ_0 [(*)]	LHV (MJ/kg)
51.6		8.9	20.5	1.2	0.14	0.49	2.76	14.4	1.35	20.39

(*) the molar amount of O2 needed for full conversion of the fuel per mole of carbon in the fuel

2.3   Ilmenite oxygen carrier

The ilmenite was provided from Titania AS. The 150 kW CLC pilot unit is designed for smaller particle size than most other CLC units. The standard ilmenite from Titania has a rather large size range of 10 – 350 µm. Before being used in the pilot unit, it has normally been sieved to about 40 – 120 µm. Some instabilities in the hydrodynamics had earlier been experienced, resulting in major plugging of the AR cyclone and downcomer. The small particle size could be a possible reason for the problem. For the SRF tests a larger size fraction of 120 – 200 µm was therefore used.

The gas flow capacity of the unit is large enough to handle this larger particle size fraction, but direct comparison with earlier biomass tests will be more questionable. To resolve this, the test started with biomass pellets and was after a while shifted over to SRF pellets, on the same test day and with almost identical operating conditions. This will allow a direct comparison of results with the biomass pellets and the SRF pellets.

Figure 4: Sample of ilmenite 120 – 200 μm.

2.4 Performance parameters

2.4.1 Fuel carbon conversion

Since the fuel enters the FR as solid particles, the first step of the conversion is to convert it from solid to gas phase. It is therefore convenient to define the fuel carbon conversion (X_{fuel-C}), which is calculated as the ratio between the carbon leaving as gas from the FR and the carbon fed to FR with the solid fuel:

$$X_{fuel-C} = \frac{\left(x_{CO_2,FR} + x_{CO,FR} + x_{CH_4,FR} + 2x_{C_2H_y,FR}\right) F_{total,dry}^{FR}}{carbon\ in\ fuel\ feed\ to\ FR},$$

where $F_{total,dry}^{FR}$ is the total dry molar flow rate of gas out of FR (kmol/h), and x_i is the mole fraction of carbon-containing gaseous species in the dry gas out of the FR. Fuel carbon conversion represents the percentage of fuel carbon that is leaving the FR in gaseous form by devolatilization, gasification and combustion in the FR. The remaining carbon will leave in the form of particulates or tar, either following the FR outlet gas, or following the OC over to the AR (contributing to CO_2 loss from the AR which will reduce the CO_2 capture rate).

2.4.2 Oxygen demand and gas conversion efficiency

The gases leaving the fuel reactor will normally not be fully converted, causing the need for an "oxygen polishing" step just downstream of the fuel reactor. I.e., pure oxygen is fed to the hot exhaust stream to completely burn out remaining unconverted fuel components. The oxygen needed for the polishing step is commonly evaluated using the so-called fuel reactor gas oxygen demand Ω_{OD}. It represents the ratio of the additional oxygen needed to completely convert the unconverted gases leaving the FR, to the stoichiometric amount of oxygen needed to fully convert all the combustible gases released in the FR. In our case the FR gas oxygen demand is calculated as

$$\Omega_{OD} = \frac{0.5x_{CO,FR} + 2x_{CH_4,FR} + 0.5x_{H_2,FR} + 3x_{C_2H_y,FR}}{\Phi_0 \left(x_{CO_2,FR} + x_{CO,FR} + x_{CH_4,FR} + 2x_{C_2H_y,FR}\right)},$$

where Φ_0 represents the molar amount of O_2 needed for full conversion of the fuel per mole of carbon in the fuel, x_i represents the mole fractions of the different species in the fuel reactor dry outlet gas, and the parenthesis in the denominator gives the total mole of carbon in the FR outlet gases. The Micro-GC gives the sum of some C_2 molecules. It is here assumed they are C_2H_4 on average.

This way of calculating the oxygen demand is a very convenient parameter as it can be calculated only from the gas analysis of the FR exhaust. However, in solid fuel CLC, there might be some losses of unconverted solid fuel particles out from the FR, mainly carbon-rich char. They should be converted in the oxygen polishing step as well, to reduce fuel losses and increase the CO_2 capture rate of the system. The above oxygen demand calculation does not include this potential fuel loss, which would increase the oxygen demand to a higher value than given by the formula above. The calculation does not take heavier hydrocarbons and tars into

account either. This would also increase the oxygen demand compared to calculated. The influence of these is considered small, which was confirmed by visual inspection of the exhaust system and filter, and FTIR gas analysis used in some of the experiments.

From the FR gas oxygen demand calculation, the FR gas conversion efficiency can be defined as

$$\eta_{gas} = 1 - \Omega_{OD} \,.$$

This represents the efficiency of the conversion of the fuel gases being released by devolatilization and gasification from the solid fuel in the FR. It should be as high as possible, ideally 100 %. However, even though it would reach 100 %, the total fuel conversion in the FR might still be less than 100 % since some fuel will leave the FR as particulates (char) as discussed above.

Another convenient parameter giving more information about the degree of fuel conversion, is the CO/CO_2 ratio. This is just the ratio between the measured CO and CO_2 concentrations out from the FR. It is less comprehensive and informative than the fuel reactor gas conversion efficiency described above. However, it is very easy to calculate and requires less gas measurements and will still provide some useful information about how well the combustible gases generated in the FR are converted.

2.4.3   CO₂ capture rate

In addition to char leaving together with the FR exhaust, there may also be a loss of char particles from the FR to the AR, following the oxygen carrier particle stream, so-called "carbon slip". These char particles will immediately be oxidized to CO_2 in the high temperature, oxygen-rich atmosphere in the AR, before the CO_2 leaves the system with the AR exhaust. Since only the CO_2 out of the FR will be captured and available for permanent storage, the CO_2 out from the AR will cause the overall CO_2 capture rate to be lower than 100%. The CO_2 capture rate is therefore calculated as

$$\eta_{CO2\ capture} = \frac{carbon\ in\ fuel\ feed\ to\ FR - carbon\ out\ from\ AR}{carbon\ in\ fuel\ feed\ to\ FR} \,.$$

The carbon in the fuel feed is calculated from the carbon content of the fuel and the fuel feeding rate given by the screw feeder, which has been calibrated for the actual fuel. The carbon out from the AR is calculated from the total mole flow out from the AR and the measured CO_2 concentration. The total mole flow out from the AR is calculated from the total N_2 mole flow out of the AR, being equal to N_2 fed to the AR with air and fluidisation gases, and the concentrations of O_2 and CO_2 at the outlet, since they will be the only gases in addition to N_2. The capture rate calculated this way considers CO_2 out from the AR as the only carbon not being captured. I.e., it requires that all unburnt gaseous components and char out from the FR is converted to CO_2 in the oxygen polishing step.

The pilot unit at SINTEF Energy Research, originally designed for gaseous fuels, does not have a carbon stripper and some char will be lost from the FR to the AR, especially through the lifter. CLC systems for solid fuels will normally be equipped with a carbon stripper to convert most of these char particles before they reach the AR, thereby increasing the capture rate of the system. Especially for slowly reacting fuels, such as petcoke, this is important. However, the

experience is that the pilot unit at SINTEF Energy Research can achieve high capture rates for biomass fuels, even without a carbon stripper. This study will evaluate if this is true also for SRF. Avoiding a carbon stripper will simplify the reactor system and its operation, and possibly provide efficiency benefits and cost savings.

2.4.4   *Oxygen carrier circulation and inventory*

There is no direct way of measuring the oxygen carrier circulation rate between the reactors in the SINTEF pilot unit. One way to estimate it, is to use the reactor pressure recordings in the AR riser. A theoretical riser mass flow can be estimated by the pressure difference (Δp) between the two upper pressure transducers, the difference in height between the transducers (Δh), the superficial gas velocity (u_0), the terminal velocity of the OC particles (u_t), the reactor riser flow area (A), and gravitational acceleration (g)

$$\dot{m}_{riser} = \frac{A}{g} \frac{\Delta p}{\Delta h} (u_0 - u_t)$$

This theoretical riser OC mass flow is not the same as the actual oxygen carrier circulation rate, since only a fraction of the particles flowing upwards in the AR riser follows the gas flow into the cyclone and is transferred to the fuel reactor. As the flow is in the turbulent to fast fluidisation regime and not in the transport regime, a large share of the particles falls downwards along the reactor wall forming an internal recirculation. Studies by Chalmers report that the share of particles leaving the reactor was about 29 % in one case and as low as 8 % in another case ([24], [25]). They point out that this fraction is expected to be different for different reactor designs, superficial velocity, and concentration. However, the calculated theoretical AR riser mass flow can be used as a good indication of the relative differences in solid circulation between different cases tested in the SINTEF pilot unit.

The oxygen carrier inventory in the two reactors and lifter is estimated by calculating the average solid-gas mixture density between subsequent pressure transducers using the pressure difference (Δp) and height between the transducers (Δh). The densities are multiplied by the volume between the pressure transducers and summed to give the OC inventory of each reactor and the lifter.

3   Results from first tests with SRF

3.1   Overview of operation

First, a heat-up sequence where electric heaters are used for inlet air streams, while propane and hydrogen is fired in both reactors, was performed. After about four hours the temperatures in the reactor system reached 1000 °C. Then, biomass pellets injection was started and the air to the FR was gradually reduced to well below stoichiometric while the hydrogen and propane flows are shut down. The temperature in the FR then drops, indicating that the ilmenite particles undergo redox reactions and that a CLC effect is present. This operating mode was maintained for 2.5 hours to activate the ilmenite oxygen carriers.

After activation was finalized, all air flow to the FR was turned off and full CLC mode was achieved. The unit was operated in full CLC mode in the time interval from 15:10 to 17:35, as seen in Figure 5. Nitrogen was used as fluidising gas in the FR for the entire period. Using Nitrogen as fluidizing gas is easier and more controllable with respect to flow amount than using steam. For fuels like biomass and SRF, which contain large shares of volatiles including hydrogen and oxygen species, steam is nevertheless produced as part of the fuel conversion process. With much less reactive fuels, such as e.g., petcoke, containing almost only carbon, steam injection is much more important to speed up gasification and conversion of the fuel.

CLC operation was first performed with biomass pellets, and thereafter with SRF from 16:35. The biomass period had several operational problems and upsets that had to be fixed. Two periods have been considered as being the best ones with respect to constant conditions. The two periods are rather short, about 8-9 minutes each.

The CLC period with SRF was much more stable, but this was probably by accident since biomass has shown to be very stable during previous campaigns. An interval of nearly 24 minutes have been evaluated. In this period, no valves or other parameters were changed at all, and the system were operating smooth and steadily by all means.
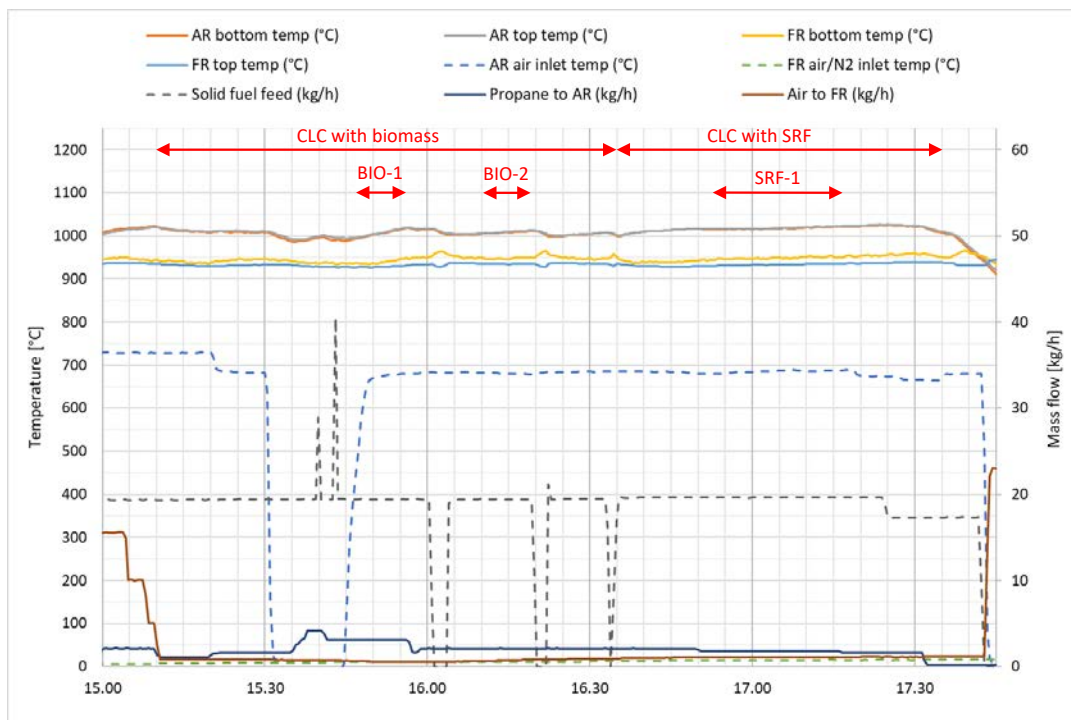
Figure 5: CLC period and time periods evaluated for biomass and SRF operation. (Note: Air to FR is zero even though the curve indicates a small amount due to a deviation of the zero-point reading of the valve.)

It was a target to keep as equal conditions as possible during operation with biomass and SRF. The main operating parameters and measurements are shown in Table 3, confirming rather equal conditions between the three periods. The largest difference is in the excess air amount, since the air flow to the AR was kept constant while SRF needs more oxygen for full combustion than the biomass fuel. It should be noted that some propane firing in the AR was needed (cf. Table 3) to maintain high enough temperatures. Especially during the biomass

period, which encountered several upsets in the fuel injection. The AR propane could be gradually reduced during the CLC period, which can indicate that the ilmenite inventory was not fully activated during the activation period and that further operation in full CLC mode was needed.

Table 3: Main operating parameters and measured values. Time average for each period.

		BIO-1	BIO-2	SRF-1
Main operating parameters				
Solid fuel feed rate	kg/h	19,4	19,4	19,6
Solid fuel power	kWth	102,5	102,4	111,2
Air inlet flow	kg/h	193	193	193
Overall air excess - λ	---	1,61	1,61	1,21
Primary air preheat temp.	°C	665	681	685
Propane firing in AR	kWth	37,8	24,7	20,7
Pressure measurements				
AR bottom pressure	mbar	107	117	126
AR loop-seal pressure	mbar	200	193	190
Lifter bottom pressure	mbar	251	243	242
FR bottom pressure	mbar	130	127	124
FR loop-seal pressure	mbar	155	161	166
Temperature measurements				
AR bottom temperature	°C	1007	1008	1017
AR top temperature	°C	1008	1009	1018
FR bottom temperature	°C	940	948	949
FR top temperature	°C	929	935	933
Gas concentration measurements				
FR CO2	vol% dry	34,9	34,8	30,0
FR CO	vol% dry	9,1	9,0	6,6
FR H2	vol% dry	3,5	3,4	4,3
FR CH4	vol% dry	3,4	3,4	4,6
FR C2H2-C2H4	vol% dry	0,6	0,6	1,4
FR O2	vol% dry	0,0	0,0	0,0
FR N2	vol% dry	48,2	48,7	53,0
AR CO2 (solid fuel + propane)	vol% dry	3,4	2,4	1,9
AR CO2 (only from solid fuel)	vol% dry	0,1	0,3	0,1
AR O2	vol% dry	8,8	10,6	10,4

3.2 Main results

The main results and performance parameters are shown in Table 4 and Figures 6 and 7. Capture rate and FR gas conversion efficiency is about the same for the SRF case as for the biomass cases. For the FR carbon conversion, the difference is significantly larger. In the SRF case, 86.5 % of the carbon in the SRF fuel is converted to carbon-containing gases (CO_2, CO, CH4, etc.), while the biomass cases show about 98 %. This means that more carbon particulates and tars leave the FR in the SRF case. The carbon particulates (char) can go to the AR or out the FR exhaust line. Since the capture rate is high in the SRF case, as high as for biomass, little of the

char is transported to the AR. I.e., there seems to be more carbon-containing particulates leaving the FR when operating on SRF compared to biomass (cf. Figure 7).

Table 4: Time averaged performance parameters, inventories, riser mass flow, and carbon balance.

		BIO-1	BIO-2	SRF-1
Performance parameters				
Carbon capture rate	%	99,0	97,9	99,1
FR carbon conversion	%	98,5	98,0	86,5
FR gas conversion efficiency	%	70,8	71,2	68,9
FR CO/CO2 ratio	---	0,26	0,26	0,22
Oxygen carrier inventories and circulation				
AR inventory	kg	26,4	29,8	33,1
FR inventory	kg	26,8	26,2	25,4
FR specific inventory	kg/MW	261	256	228
AR riser mass flow	kg/s	3,62	3,85	3,56
Carbon balance				
Carbon fed with solid fuel	kg/h	9,84	9,83	10,14
Carbon fed with solid fuel	%	100	100	100
Carbon out of FR as gas	%	98,5	98,0	86,5
Carbon out of AR as gas	%	1,0	2,1	0,9
Sum carbon out FR + AR as gas	%	99,4	100,0	87,4
Balance = carbon out of FR as particulates	%	0,6	0,0	12,6
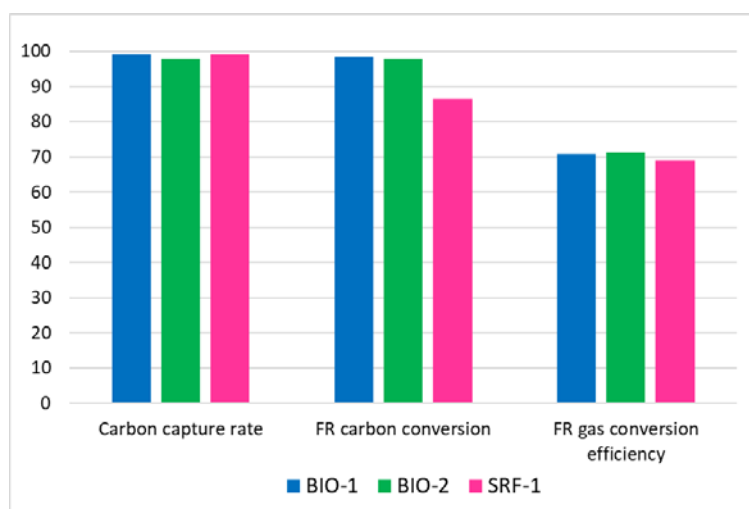
Figure 6: Capture rate, carbon conversion and gas conversion efficiency for evaluated periods.
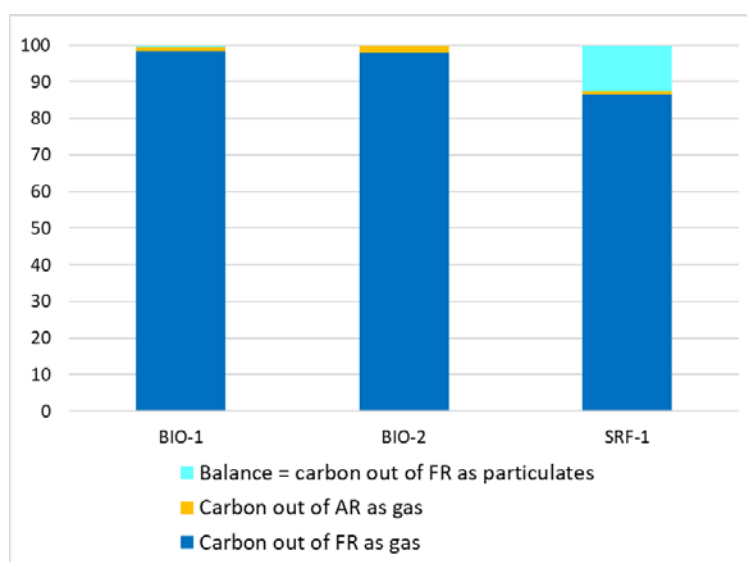
Figure 7: Carbon balance for the three evaluated period.

3.3 Comparison with earlier results

A comparison is made with some earlier tests using biomass and petcoke as fuel. In these earlier tests the ilmenite oxygen carrier was of smaller size, in the range 40 – 120 µm. The more recent results with biomass and SRF pellets presented in section 3.2 was with ilmenite size in the range 120 – 200 µm. In both cases the ilmenite was from Titania AS in Norway.

Table 5 gives the operating conditions and some performance parameters for these earlier tests. The capture rate and FR gas conversion efficiency is in addition shown in Figure 8 and Figure 9. The operating conditions are not directly comparable with the new biomass and SRF tests presented above. However, the general trend is that the earlier tests have a FR gas conversion efficiency of about 80 % in the biomass cases, both with whole pellets and when milled and sieved (< 800 µm was sieved away). I.e., about 10 %-points higher than the new bio and SRF tests. On the other hand, the earlier biomass tests show somewhat lower capture rate, about 8-9 %-points lower, but still around 90 % capture rate.

Table 5: Time averaged operating conditions and performance parameters.

		Biomass pellets	Biomass milled/sieved	Mix b/p 75/25	Mix b/p 50/50	Mix b/p 50/50 smaller
Solid fuel power	kWth	108,6	99,7	80,5	93,1	109,4
Overall air excess - λ	---	1,54	1,24	1,78	1,56	1,01
AR bottom temperature	°C	1011	1000	989	990	991
AR top temperature	°C	1019	1010	998	1001	999
FR bottom temperature	°C	996	976	973	974	966
FR top temperature	°C	977	960	960	959	954
Carbon capture rate	%	88,3	92,3	64,8	47,5	57,6
FR gas conversion efficiency	%	81,9	80,2	89,1	90,9	85,5
FR inventory	kg	27,5	12,2	20,0	22,6	28,7
FR specific inventory	kg/MW	253	122	249	243	262
AR riser mass flow	kg/s	7,4	3,4	4,7	4,8	4,8
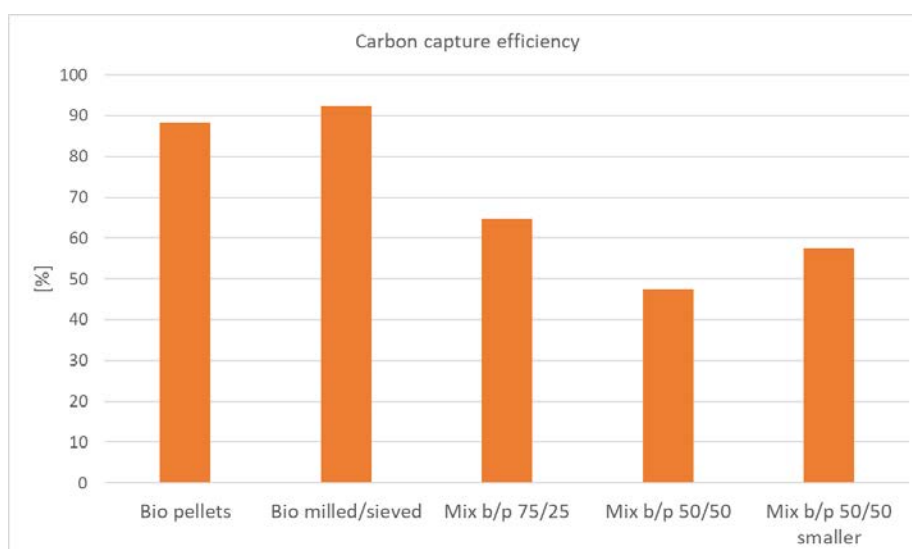
Figure 8: Carbon capture efficiency from earlier biomass and petcoke tests with ilmenite 40-120 µm.
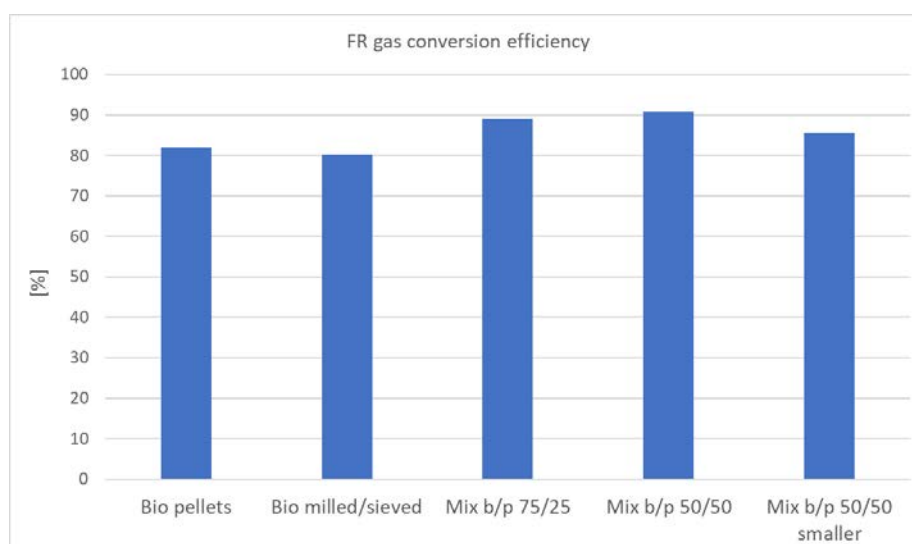
Figure 9: FR gas conversion efficiency from earlier biomass and petcoke tests with ilmenite 40-120 µm.

Some earlier cases using a mix of biomass and petcoke have also been tested. The biomass is the milled and sieved fraction whereas the petcoke had a size range of 315 – 500 µm. It was operated with a mix of 75/25 and 50/50 biomass/petcoke. In addition, the 50/50 mix was repeated using un-sieved biomass incl. the fines from milling, plus petcoke in size 100 – 315 µm, also including the fines from milling. It is clearly seen how the slow reacting petcoke fuel decreases the capture rate, but the FR gas conversion is increased since less gas is to be converted in the FR. The batch with smaller fuel particles improves the capture rate on the expense of the FR gas conversion, which is reduced.

4   Discussion and conclusion

The very first tests with SRF fuel in a CLC unit has been performed. It has been shown that the SRF fuel in the form of pellets can be injected without problems as clogging etc. The operation in CLC mode was stable with no process upsets. The carbon capture rate was very high for both the SRF case, and the reference biomass cases, about 98-99 %. The FR gas conversion efficiency was also about the same for the SRF and reference bio cases, about 70 %.

With SRF, the FR carbon conversion was lower than for biomass. For biomass it was about 98 % whereas for SRF it was 86.5 %. There are uncertainties in these results, but it does not seem likely that such large difference can be explained only be uncertainties in the measurements or the relatively short time of operation.

Compared to some earlier tests using biomass, the new results seem to give a lower FR gas conversion efficiency, about 10-% points, and a higher capture rate, about -9 %-points. This comparison is not exact since the operating conditions are not completely equal. The earlier tests used an ilmenite with smaller particle size, 40-120 µm, compared to 120-200 µm for the new tests. In general, the earlier tests showed higher FR temperatures, which can explain the higher gas conversion efficiency. The earlier tests also had slightly higher riser mass flow, indicating that the oxygen carrier circulation between the reactors were higher, which can explain the lower capture rate in the earlier biomass tests.

The earlier tests did also include mixed fuel of biomass and petcoke. The inclusion of the low reacting petcoke fuel gives a large decrease in the capture rate, which is expected since the 150 kW CLC unit does not have a carbon stripper. For the more reactive fuels as biomass and SRF, both the new and earlier results show rather high capture rate even without a carbon stripper. Especially the new tests showing very high values. Results below 95 % may not be attractive from a cost and efficiency perspective, so results closer to 90 % may not be considered good enough.

The next test campaign will be performed with longer duration and a new ilmenite oxygen carrier. The ilmenite particle size will be smaller, more equal to what has been used before. It is of interest to see if this can improve the FR carbon conversion and FR gas conversion efficiency, while still managing a high capture rate.

References

[1] IPCC (2018) Global Warming of 1.5°C. An IPCC Special Report on the impacts of global warming of 1.5°C above pre-industrial levels, IPCC

[2] IEA (2021) Net Zero by 2050 - A Roadmap for the Global Energy Sector, IEA

[3] Global CCS Institute (2021) The Global Status of CCS: 2021, Australia

[4] Rydén M., Lyngfelt A., Langørgen Ø., Larring Y., Brink A., Teire S., Havåg H., Karmhagen P. (2017), Negative CO_2 Emissions with Chemical-Looping Combustion of Biomass – a Nordic Energy Research Flagship Project, *Energy Procedia* **114**, pp. 6074-6082

[5] Spinelli M., Peltola P., Bischi A., Ritvanen J., Hyppänen T., Romano M. (2016), Process integration of chemical looping combustion with oxygen uncoupling in a coal-fired power plant, *Energy* **103**, pp. 646-659

[6] Lyngfelt A., Leckner B. (2015), A 1000 MW_{th} boiler for chemical-looping combustion of solid fuels – Discussion of design and costs. *Applied Energy* **157**, pp. 475-487

[7] Fu C., Anantharaman R., Roussanaly S., Yazdanpanah M., Laroche C., Bertholin S. (2021), CLC-CCS plant modelling - Deliverable D5.2 from the CHEERS project, https://cheers-clc.eu/results/

[8] Lindroos T.J., Rydén M., Langørgen Ø., Pursiheimoa E., Pikkarainen T. (2019), Robust decision making analysis of BECCS (bio-CLC) in a district heating and cooling grid, *Sustainable Energy Technologies and Assessments* **34**, pp. 157–172

[9] Lyngfelt A., Brink A., Langørgen Ø., Mattisson T., Rydén M., Linderholm C. (2019), 11,000 h of chemical-looping combustion operation─Where are we and where do we want to go?, *International Journal of Greenhouse Gas Control* **88**, pp. 38–56

[10] Adánez J., Abad A., Mendiara T., Gayán P., de Diego L.F., García-Labiano F. (2018), Chemical looping combustion of solid fuels, *Progress in Energy and Combustion Science* **65**, pp. 6-66

[11] Yazdanpanah M., Guillou F., Bertholin S., Zhang A. (2018), Demonstration of Chemical Looping Combustion (CLC) with Petcoke Feed for Refining Industry in a 3 MW_{th} Pilot Plant, *14th International Conference on Greenhouse Gas Control Technologies*, Melbourne, Australia

[12] Sun H., Cheng M., Chen D., Xu l., Li Z., Cai N. (2015), Experimental Study of a Carbon Stripper in Solid Fuel Chemical Looping Combustion, *Industrial & Engineering Chemistry Research* **54**, pp. 8743-8753

[13] Eriksson T., Barišić V., Nuortimo K., Jäntti T. (2015), Advanced utility CFB technology for challenging new solid biomass fuels, Amec Foster Wheeler Energia Oy, PowerGen Europe 2015

[14] Shen L., Wu J., Xiao J., Song Q., Xiao R. (2009), Chemical-Looping Combustion of Biomass in a 10 kW_{th} Reactor with Iron Oxide As an Oxygen Carrier, *Energy & Fuels* **23**, pp. 2498–2505

[15] Mendiara T., Perez-Astray A., Izquierdo M.T., Abad A., de Diego L.F., Garcia-Labiano F., Gayán P., Adánez J. (2018), Chemical Looping Combustion of different types of biomass in a 0.5 kW_{th} unit, *Fuel* **211**, pp. 868-75

[16] Schmitz M., Linderholm C. (2018), Chemical looping combustion of biomass in 10-and 100-kW pilots - Analysis of conversion and lifetime using a sintered manganese ore, *Fuel* **231**, pp. 73-84

[17] Ohlemüller P., Ströhle J., Epple B. (2017), Chemical looping combustion of hard coal and torrefied biomass in a 1 MW_{th} pilot plant, *International Journal of Greenhouse Gas Control* **65**, pp. 149-159

[18] Langørgen Ø., Saanum I. (2018), Chemical Looping Combustion of wood pellets in a 150 kW_{th} CLC reactor. *International Conference on Negative CO_2 Emissions*, Göteborg

[19] Anthony E.J. (1995), Fluidized-bed combustion of alternative solid fuels – Status, successes and problems of the technology, *Progress in Energy and Combustion Science* **21**(3), pp. 239-68

[20] Van Caneghem J., Brems A., Lievens P., Block C., Billen P., Vermeulen I., Dewil R., Baeyens J., Vandecasteele C. (2012), Fluidized bed waste incinerators: Design, operational and environmental issues, *Progress in Energy and Combustion Science* **38**(4), pp. 551-582

[21] De Gisi S., Chiarelli A., Tagliente L., Notarnicola M. (2018), Energy, environmental and operation aspects of a SRF-fired fluidized bed waste-to-energy plant, *Waste Management* **73**, pp. 271–286,

[22] Bischi A., Langørgen Ø., Saanum I., Bakken J., Seljeskog M., Bysveen M., MorinJ.X., Bolland O. (2011), Design study of a 150kW_{th} double loop circulating fluidized bed reactor system for chemical looping combustion with focus on industrial applicability and pressurization, *International Journal of Greenhouse Gas Control* **5**, pp. 467-474

[23] Langørgen Ø., Saanum I., Haugen N.E.L. (2017), Chemical looping combustion of methane using a copper-based oxygen carrier in a 150 kW reactor system, *Energy Procedia* **114**, pp. 352-360

[24] Markström P., Lyngfelt A. (2012) Designing and operating a cold-flow model of a 100 kW chemical-looping combustor, *Powder Technology* **222**, pp. 182-192.

[25] Markström P., Linderholm C., Lyngfelt A. (2014), Operation of a 100 kW chemical-looping combustor with Mexican petroleum coke and Cerrejón coal, *Applied Energy* **113**, pp. 1830-1835